PHYSICAL REVIEW B **94**, 241113(R) (2016)

Lifshitz transition driven by spin fluctuations and spin-orbit renormalization in $NaOsO_3$

Bongjae Kim,[1] Peitao Liu,[1] Zeynep Ergönenc,[1] Alessandro Toschi,[2] Sergii Khmelevskyi,[1,3] and Cesare Franchini[1,*]

[1]*University of Vienna, Faculty of Physics and Center for Computational Materials Science, Vienna 1090, Austria*

[2]*Institut für Festkörperphysik, Technische Universität Wien, Vienna 1040, Austria*

[3]*Institute for Applied Physics, Technische Universität Wien, Vienna 1040, Austria*

(Received 13 January 2016; revised manuscript received 21 November 2016; published 21 December 2016)

In systems where electrons form both dispersive bands and small local spins, we show that changes in the spin configuration can tune the bands through a Lifshitz transition, resulting in a continuous metal-insulator transition associated with a progressive change in the Fermi surface topology. In contrast to the Mott-Hubbard and Slater pictures, this spin-driven Lifshitz transition appears in systems with a small electron-electron correlation and large hybridization. We show that this situation is realized in 5*d* distorted perovskites with half-filled t_{2g} bands such as $NaOsO_3$, where the strong *p-d* hybridization reduces the local moment, and spin-orbit coupling causes a large renormalization of the electronic mobility. This weakens the role of electronic correlations and drives the system towards an itinerant magnetic regime which enables spin fluctuations.

DOI: 10.1103/PhysRevB.94.241113

Metal-to-insulator transitions (MITs) are one of the most important phenomena in solid-state physics and their fundamental understanding represents an enduring challenge in solid-state theory [1,2]. Different mechanisms have been invoked to explain the formation of an insulating regime. Classical examples are realized in 3*d* transition metal oxides (TMOs), where the nonconducting state is typically understood within the Mott-Hubbard model as arising from the competition between a strong electron-electron interaction (U) and the electronic mobility, associated with the (noninteracting) bandwidth (W) [3–5]. When moving to the more spatially extended 4*d* and 5*d* orbitals, the W increases and the U is expected to become smaller, leading to a tendency towards metallicity as in the itinerant magnet $SrRuO_3$ [6]. In contrast to these expectations, recent theory and experiment have revealed that in "heavy" 5*d* TMOs, the enhanced spin-orbit coupling (SOC) strength [7] can lead to the formation of a variety of novel types of quantum states, including unexpected insulating regimes [8–11]. In the most representative example, Sr_2IrO_4, the concerted action of a strong SOC and a moderate U leads to the opening of a small spectral gap called the *relativistic Mott* gap [11–13]. Other and rarer types of MITs have been recently proposed for magnetic relativistic osmium oxides based on the Slater mechanism [14–17], driven by antiferromagnetic (AFM) order, where the gap is opened by exchange interactions and not by electronic correlations [18], or Lifshitz-like processes [19,20], involving a rigid change of the Fermi surface topology [21].

In this Rapid Communication we show that in weakly correlated (small U) itinerant magnets, the combined effect of longitudinal and rotational spin fluctuations can cause a continuous MIT with Lifshitz characteristics, fundamentally different from relativistic Mott or purely Slater insulating states. The necessary conditions for the onset of this type of spin-driven Lifshitz MIT are the coexistence of a small U, a small local moment, and a high degree of orbital hybridization. This places the system at the border of a magnetic and electronic instability where a Lifshitz MIT is possible. This situation can be realized in structurally distorted, nominally half-filled t_{2g}^3 5*d* oxides such as $NaOsO_3$ and $Cd_2Os_2O_7$ or iridates. By taking $NaOsO_3$ as a prototypical example, we show that here the balance between U and W is controlled by the SOC: The SOC induces a surprisingly large reduction of electronic mobility which renormalizes the U and pushes the system into a weakly correlated and magnetically itinerant regime subjected to spin fluctuations. We find that at high temperatures, $NaOsO_3$ is a paramagnetic metal, but as the temperature decreases, the changes in the amplitude and direction of the spins lead to the continuous vanishing of holes and electrons pockets in the Fermi surface (FS), that do not involve any substantial modification of the underlying band structure [21], consistent with a Lifshitz-type MIT.

Experimental observations indicate that $NaOsO_3$ undergoes a second-order MIT concomitant with the onset of an antiferromagnetic long-range ordering at a Néel temperature (T_N) of ≈ 410 K. This behavior is apparently adaptable to a Slater mechanism [14–17,22]. However, the bad-metal behavior observed in a wide intermediate temperature region ($0.1T_N < T < T_N$) [14], the Curie-Weiss behavior of the susceptibility above T_N, and the need for a sizable U in density functional theory (DFT) calculations to open the gap, is in conflict with an authentic Slater mechanism [22–24].

The fundamental properties of $NaOsO_3$ have been clearly exposed by Jung *et al.* [22]. In particular, it was shown that the apparent discrepancy between the measured Os ordered moment of only $1\mu_B$ [15] and the nominal t_{2g}^3 ($L_{\text{eff}} = 0$) configuration should be attributable to the large *p-d* hybridization that effectively reduces the local moment and forms an (electronic and magnetic) itinerant background [22]. However, the authors concluded that the role of SOC is modest in this system, since the $L_{\text{eff}} = 0$ state should exhibit a negligible orbital moment. In the following, we will show that relativistic effects can be strong even in a quenched orbital moment scenario, and we will explain that the SOC is the crucial effect in paving the way for a continuous MIT in $NaOsO_3$.

Spin-orbit-induced renormalization. We begin by studying the effects of U and its interplay with the SOC. All calculations were performed using the Vienna *ab initio* simulation

*cesare.franchini@univie.ac.at

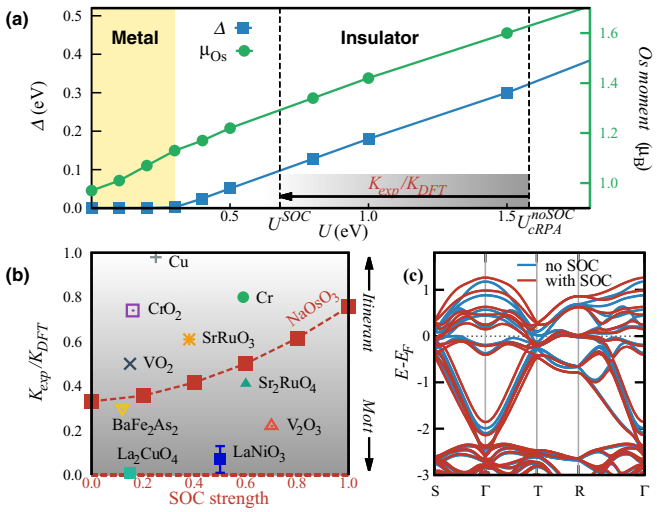

FIG. 1. Relativistic "renormalization" of the electronic correlation. (a) Energy gap and Os magnetic moment. (b) $K_{\rm expt}/K_{\rm DFT}$ as a function of the SOC strength for $NaOsO_3$ and other reference systems. The measured data of the electron mobility are taken from Ref. [16] ($NaOsO_3$), Ref. [27] ($LaNiO_3$), and Ref. [28] (all other materials). (c) Paramagnetic band structure of $NaOsO_3$ with and without SOC.

package (VASP) [25] using the DFT+U method and including relativistic effects (see the Supplemental Material [26]).

As usual, the values of the experimentally accessible observables such as the spectral gap Δ and the magnetic moment $\mu_{\rm Os}$ are highly sensitive to the choice of U, as visualized in Fig. 1(a). For $U = 0$, $NaOsO_3$ is metallic, but for $U \geqslant 0.3$ eV it exhibits a finite gap that increases linearly with U. The experimentally reported low-temperature optical gap, 0.1 eV [16], and $\mu_{\rm Os} \approx 1\mu_B$ [14] clearly indicate that the optimal value of U should be chosen around 0.5 eV. At the same time, if we calculate U entirely *ab initio* within the constrained random phase approximation (cRPA) [29], neglecting all relativistic effects (SOC = 0), we obtain $U^{\rm no\ SOC} = 1.58$ eV, a value similar to the one used in previous studies (i.e., $U = 2$ eV [22–24]). As we demonstrate here, the root of this apparent controversy lies in the surprising "competition" between SOC and electronic correlation.

We study the interplay between SOC and correlation by comparing our DFT+U results with available infrared optical experiments. One rather general way [28,30,31] to estimate the degree of electronic correlation of a system is to evaluate the reduction of the electronic kinetic energy (mass renormalization) due to Coulomb repulsion. This can be quantified by the ratio $K_{\rm expt}/K_{\rm DFT}$ between the experimentally measured kinetic energy ($K_{\rm expt}$), determined by integrating over frequency the Drude contribution in the optical conductivity σ_D and the corresponding "noncorrelated" kinetic energy $K_{\rm DFT}$ obtained by DFT at $U = 0$. Considering that σ_D can be expressed in terms of the plasma frequency ω_p via $\int d\omega\, \sigma_D(\omega) = \omega_p^2/8$, one can rewrite the kinetic energy ratio as

$$\frac{K_{\rm expt}}{K_{\rm DFT}} = \frac{\omega^2_{p,\rm expt}}{\omega^2_{p,\rm DFT}}. \qquad (1)$$

Surprisingly, $K_{\rm expt}/K_{\rm DFT}$ in $NaOsO_3$ is dramatically dependent on the SOC strength, as shown in Fig. 1(b). Without SOC, one should have classified the system as intermediate-strong correlated with $K_{\rm expt}/K_{\rm DFT} = 0.33$, which is close to Fe-pnictide superconductors. As SOC is considered in the DFT calculations, however, $K_{\rm DFT}$ gets systematically reduced, as the estimated degree of correlation. For a full inclusion of SOC (SOC = 1) we obtain $K_{\rm expt}/K_{\rm DFT} = 0.76$, as in conventional metals (Cr). $NaOsO_3$ represents a system where such a strong renormalization of the balance between SOC and correlations is reported.

Supporting evidence for the importance of SOC is provided by the computed SOC energy, 0.4 eV/Os, and by comparing the electronic structure with and without SOC [Fig. 1(c)]. The inclusion of SOC leads to a widening of the bandwidth by about 0.3 eV, a linearization of the band near Γ which yields the formation of a Dirac-like feature and, most importantly for the electron mobility, a band flattening near E_F that increases the effective masses and decreases $K_{\rm DFT}$.

Therefore, by turning on the SOC, the estimated degree of correlation moves gradually from the border to the Mott physics to the one of conventional metallic systems. This significant relativistic renormalization clarifies the origin of the above-mentioned inconsistencies on the value of U in this system. More quantitatively, by rescaling the cRPA value of $U^{\rm no\ SOC}$ by the SOC-induced renormalization factor [31], we obtain $U^{\rm SOC} = 0.68$ eV (comparable to the SOC energy), which leads to a much better description of the band gap [see the arrow in Fig. 1(a)]. This smaller value of U is also consistent with the U proposed for similar compounds such as $LiOsO_3$, $U < 1$ eV [32], and the itinerant magnet $SrRuO_3$, $U \approx 0.6$ eV [33].

Importantly, the analogy with $SrRuO_3$ is not limited to the low degree of correlation but also involves the magnetic itinerancy. Although $NaOsO_3$ exhibits a high $T_N = 410$ K, the effective moment extracted from the Curie-Weiss behavior of the high-temperature susceptibility, $2.71\mu_B$ [14], is much higher than the ground state magnetic moment measured by neutron diffraction, $\approx 1\mu_B$ [15]. This indicates a large Rhodes-Wohlfarth ratio and is suggestive of an itinerant antiferromagnetic behavior [34]. This magnetic itinerancy would *not* be compatible with a large U and is essential to explain the MIT, as discussed below.

Spin fluctuations and Lifshitz MIT. After clarifying the crucial role played by SOC to reduce the electron correlation, we are ready to address the most intriguing feature of this compound—the origin of the continuous MIT at finite temperatures.

Our main results are summarized in Figs. 2 and 3. First, we recall that the resistivity (ρ) curve of $NaOsO_3$ [Fig. 3(a)] shows two anomalies: one at $T_N = 410$ K, corresponding to a sudden increase of ρ, and the second one at around $T_A = 30$ K ($T/T_N \approx 0.1$) [14,15], characterized by a steeper increment. The region below T_A has a clear insulatinglike behavior with a large and rapidly growing ρ, whereas in the intermediate region, $T_A < T < T_N$, ρ is always smaller than 1 Ω cm and grows more slowly, with a bad-metal/pseudogap behavior. The bad-metal state is compatible with the observations that the optical conductivity does vanish at T_N and does not show a clear downturn at low frequencies in the intermediate-temperature

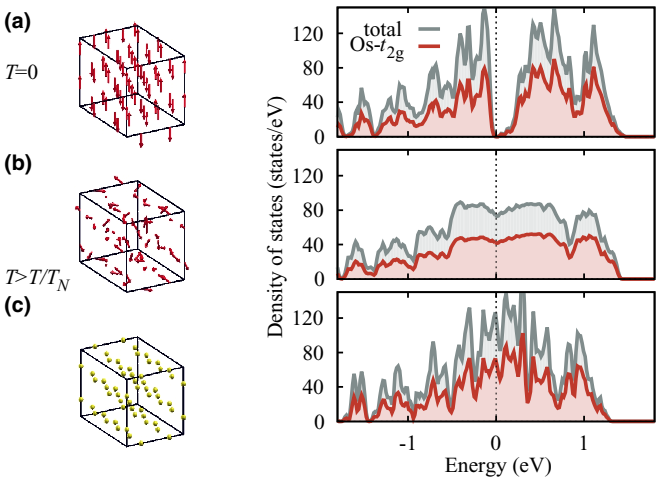

FIG. 2. High-temperature paramagnetic state. Total and t_{2g} projected density of states (DOS) of the (a) low-temperature insulating AFM ground phase, (b) disordered paramagnetic phase (metallic), and (c) nonmagnetic phase (metallic). The arrows indicate the Os spins.

region [16]. This is very unusual for TMOs, where—in the presence of a Mott-Hubbard MIT—the opposite trend can be observed [35]. Similar temperature dependence properties were reported, instead, for the narrow-gap semiconductor FeSi: At low temperatures, FeSi is a paramagnetic insulator but it develops a pseudogap associated with a bad-metal state as the temperature increases [36–38]. This anomalous behavior is explained well by spin fluctuations in the context of the Moriya theory of itinerant magnetism [39]. This similarity is of course very inspiring for the identification of the physical mechanisms at play in $NaOsO_3$.

To substantiate this idea we explore the effect of transverse (rotational) and longitudinal spin fluctuations using magnetically constrained noncollinear DFT [13]. As a first step, we have modeled the effect of rotational spin fluctuations in the high-temperature spin disordered configuration using large supercells containing 32 Os sites, starting from randomly rotated Os spin moments in a paramagnetic arrangement (i.e., the total magnetic moment is zero), by fixing the magnitude of the magnetic moments to the ground state value. The results are summarized in Fig. 2. The starting point is the density of states (DOS) of the reference collinear AFM insulating state at $T = 0$ [Fig. 2(a)]. The paramagnetic DOS [Fig. 2(b)] clearly shows that above T_N the system is an ordinary metal, independently of the value of the local magnetic moment. By allowing a full relaxation of the moments, the noncollinear paramagnetic state converges to a unrealistic metallic non-spin-polarized state [Fig. 2(c)] with entirely quenched local spin moments, similarly to the case of other magnetically itinerant metals such as Cr and Ni [40]. However, longitudinal spin fluctuations induce local moments forming the true, realistic, high-temperature paramagnetic state [41]. Thus, to explain the double anomaly behavior in the resistivity curve at finite temperatures [Fig. 3(a)], the effect of both rotational and longitudinal spin fluctuations should be taken into account. To quantify the amplitude of the moments induced by longitudinal spin fluctuations at finite temperatures, we employ the phenomenological theory of Moriya, as described below [39].

Within spin-fluctuation theory there is a universal relation between the magnitude of the local mean square fluctuating magnetic moment at the transition temperature ($M = \sqrt{\langle M^2(T_N)\rangle}$) and the ground state local moment (M_0) expressed by the Moriya formula $\langle M^2(T_N)\rangle = \frac{3}{5}M_0^2$ [34,39]. By combining the Moriya formula with the Mohn and Wohlfarth approximation [34], which assumes a linear temperature dependence of the local mean square moment amplitude, we arrive at the following relation between the amplitude of the fluctuating Os moment [$M(T)$] and temperature:

$$M(T) = M_0\sqrt{1 - \frac{2}{5}\frac{T}{T_N}}. \qquad (2)$$

Using this relation we have conducted a series of calculations with fixed magnetic moments from $\mu_{Os} = M_0 = 1.2\mu_B$ to $0\mu_B$ to examine the changes of the electronic structure upon temperature. The results are collected in Fig. 3. At $T = 0$ (top panels) the system is an antiferromagnetic insulator with a narrow band gap and an Os moment $\mu_{Os} = 1.17\mu_B$. As the temperature increases, the resistivity curve shows its first anomaly at $T_A = T/T_N \approx 0.1$ [Fig. 3(a)], corresponding to the closing of the indirect band gap Δ_i due to longitudinal spin fluctuations that pushes down the conduction band minima at the Y point [Fig. 3(c)]. Right above T_A, the system starts to develop a FS [Fig. 3(d)] and enters a bad-metal state characterized by several hole and electron pockets with a pseudogap [PS, see Fig. 3(e)] separating the valence and conduction bands. This pseudogap (Δ_d) decreases with temperature and finally closes for $M(T) = \mu_{Os} = 0.9\mu_B$ at about $T \simeq T_N$, the second anomaly in the resistivity curve indicated by an arrow in Fig. 3(a). This second anomaly, due to the rotational magnetic disorder described previously, set the transition to a metallic behavior for $T > T_N$. The entire process is sketched schematically in Fig. 3(e). By considering the evolution of the electronic band structure [Fig. 3(c)], we finally gain a complete description of the MIT in $NaOsO_3$. The bands change almost rigidly with temperature and lead to a continuous change of the FS topology in terms of the appearance of progressively larger hole and electron pockets [Fig. 3(d)]: This represents a clear hallmark of a Lifshitz transition [20,21].

Discussion. Lifshitz transitions such as the one described here are likely to be relevant for other magnetic materials lying at the border between a localized Mott picture and a metallic regime such as NiS [42], or 5d TMOs with a nominally half-filled t_{2g}^3 configuration such as $Cd_2Os_2O_7$ [19,20], Ba_2YOsO_6 [43], and d^3 iridates. Half-filled t_{2g}^3 systems, in fact, appear particularly suitable for a Lifshitz MIT, because this configuration leads to an "optimum" balance between hybridization and electron-electron correlations. This is mostly due to the relativistic effects on the band structure: For less than half-filled situations the SOC induces a relevant splitting of the band, which induces a substantial magnification of the effects of the electronic correlation (U), yielding to relativistic Mott states such as the ones observed in Ba_2NaOsO_6 (d^1) and Ba_2CaOsO_6 (d^2) [43], whereas for more

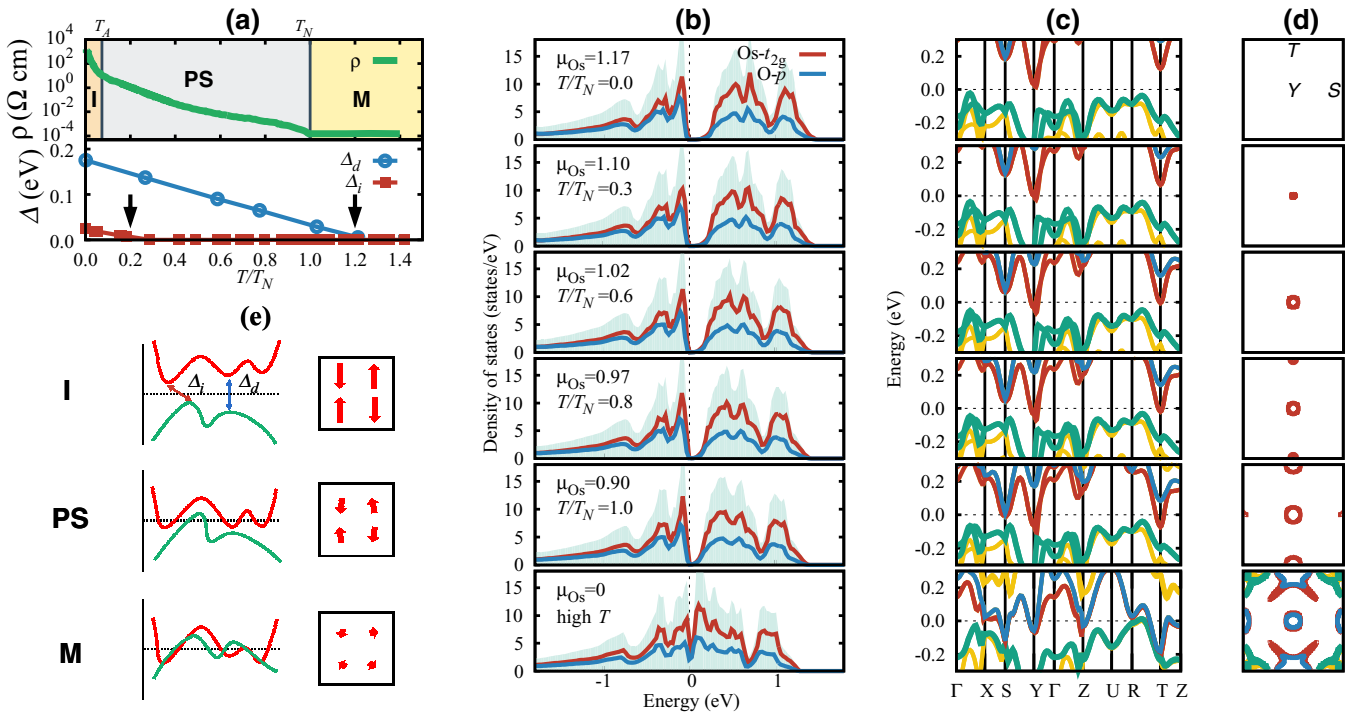

FIG. 3. Temperature-dependent MIT. (a) Indirect band gap (Δ_i) and direct pseudogap (Δ_d) as a function of temperature compared with the experimental resistivity curve readapted from Ref. [14]. The two anomalies in the resistivity curves at T_A and T_N set the transition from an insulating (I) to a pseudogap (PS) state and from the PS to a purely metal (M) state, respectively. These two anomalies are correlated with the closing of the insulating gaps (Δ_i) and the pseudogaps (Δ_d) (indicated by arrows). (b) Partial DOS, (c) band structure, and (d) FS for different temperatures (T/T_N) corresponding to different Os magnetic moments μ_{Os} [Eq. (2)]. (e) Schematic diagram of the MIT. I: AFM insulator; PS: AFM pseudogap state with longitudinal (and small rotational) spin fluctuation; M: magnetically itinerant metal.

than half-filled occupations the bandwidth increases, leading to a metallic solution (d^4 $BaOsO_3$ and $NaIrO_3$ [44]). For an ideally half-filled occupation, on the other hand, the orbital moment is almost completely quenched and the SOC does not lead to substantial band splitting. Rather, according to our study, it causes a *reduction* of the effective electron-electron correlation, which weakens significantly the tendency towards relativistic Mott states, and paves the way for a completely different physics, which is radically different from the trends typically observed in 3*d* and 4*d* TMOs.

Conclusions. In summary, we have shown that the coexistence of weak electronic correlation and itinerant magnetism can lead to a spin-driven Lifshitz MIT, i.e., a magnetically induced continuous reconstruction of the Fermi surface. For $NaOsO_3$ we found that the MIT is prompted by transverse and longitudinal fluctuations of the itinerant Os moments, and is intimately bound to the SOC-driven renormalization of the electronic kinetic energy. Our study explains the three different regimes observed experimentally: (i) At low T, $NaOsO_3$ is an AFM insulator; (ii) at $T = T_A$, it enters a bad-metal regime due to longitudinal spin fluctuations; and, finally, (iii) at $T = T_N$, rotational spin fluctuations close the direct pseudogap and the system becomes a paramagnetic metal. Spin fluctuations and the tunability by doping and pressure of the Lifshitz FS reconstruction could give rise to different magnetic, orbital, and superconducting transitions, to be exploited for engineering TMO-based heterostructures. Moreover, the surprising role played by the SOC in $NaOsO_3$, as well as its "competitive" action against correlations, could radically affect the theoretical description of the relativistic mechanisms controlling the electronic properties of many other oxides.

Acknowledgments. We thank A. Perucchi, S. Lupi, and L. Boeri for helpful discussions. This work was supported by the joint Austrian Science Fund (FWF) and Indian Department of Science and Technology (DST) project INDOX (I1490-N19), and by the FWF-SFB ViCoM (Grant No. F41). Computing time at the Vienna Scientific Cluster is greatly acknowledged.

[1] N. F. Mott, Metal-insulator transition, Rev. Mod. Phys. **40**, 677 (1968).

[2] M. Imada, A. Fujimori, and Y. Tokura, Metal-insulator transitions, Rev. Mod. Phys. **70**, 1039 (1998).

[3] E. Dagotto, Complexity in strongly correlated electronic systems, Science **309**, 257 (2005).

[4] Y. Tokura and N. Nagaosa, Orbital physics in transition-metal oxides, Science **288**, 462 (2000).

[5] G. Kotliar and D. Vollhardt, Strongly correlated materials: Insights from dynamical mean-field theory, Phys. Today **57** (3), 53 (2004).

[6] G. Koster, L. Klein, W. Siemons, G. Rijnders, J. S. Dodge, C.-B. Eom, D. H. A. Blank, and M. R. Beasley, Structure, physical properties, and applications of $SrRuO_3$ thin films, Rev. Mod. Phys. **84**, 253 (2012).

[7] G. Cao, J. Bolivar, S. McCall, J. S. Crow, and R. P. Guertin, Weak ferromagnetism, metal-to-nonmetal transition, and negative differential resistivity in single-crystal Sr_2IrO_4, Phys. Rev. B **57**, R11039(R) (1998).

[8] Y. K. Kim, N. H. Sung, J. D. Denlinger, and B. J. Kim, Observation of a *d*-wave gap in electron-doped Sr_2IrO_4, Nat. Phys. **12**, 37 (2016).

[9] G. Jackeli and G. Khaliullin, Mott Insulators in the Strong Spin-Orbit Coupling Limit: From Heisenberg to a Quantum Compass and Kitaev Models, Phys. Rev. Lett. **102**, 017205 (2009).

[10] D. Pesin and L. Balents, Mott physics and band topology in materials with strong spin-orbit interaction, Nat. Phys. **6**, 376 (2010).

[11] B. J. Kim, H. Jin, S. J. Moon, J.-Y. Kim, B.-G. Park, C. S. Leem, J. Yu, T. W. Noh, C. Kim, S.-J. Oh, J.-H. Park, V. Durairaj, G. Cao, and E. Rotenberg, Novel $J_{\rm eff} = 1/2$ Mott State Induced by Relativistic Spin-Orbit Coupling in Sr_2IrO_4, Phys. Rev. Lett. **101**, 076402 (2008).

[12] C. Martins, M. Aichhorn, L. Vaugier, and S. Biermann, Reduced Effective Spin-Orbital Degeneracy and Spin-Orbital Ordering in Paramagnetic Transition-Metal Oxides: Sr_2IrO_4 Versus Sr_2RhO_4, Phys. Rev. Lett. **107**, 266404 (2011).

[13] P. Liu, S. Khmelevskyi, B. Kim, M. Marsman, D. Li, X.-Q. Chen, D. D. Sarma, G. Kresse, and C. Franchini, Anisotropic magnetic couplings and structure-driven canted to collinear transitions in Sr_2IrO_4 by magnetically constrained noncollinear DFT, Phys. Rev. B **92**, 054428 (2015).

[14] Y. G. Shi, Y. F. Guo, S. Yu, M. Arai, A. A. Belik, A. Sato, K. Yamaura, E. Takayama-Muromachi, H. F. Tian, H. X. Yang, J. Q. Li, T. Varga, J. F. Mitchell, and S. Okamoto, Continuous metal-insulator transition of the antiferromagnetic perovskite $NaOsO_3$, Phys. Rev. B **80**, 161104(R) (2009).

[15] S. Calder, V. O. Garlea, D. F. McMorrow, M. D. Lumsden, M. B. Stone, J. C. Lang, J. W. Kim, J. A. Schlueter, Y. G. Shi, K. Yamaura, Y. S. Sun, Y. Tsujimoto, and A. D. Christianson, Magnetically Driven Metal-Insulator Transition in $NaOsO_3$, Phys. Rev. Lett. **108**, 257209 (2012).

[16] I. Lo Vecchio, A. Perucchi, P. Di Pietro, O. Limaj, U. Schade, Y. Sun, M. Arai, K. Yamaura, and S. Lupi, Infrared evidence of a Slater metal-insulator transition in $NaOsO_3$, Sci. Rep. **3**, 2990 (2013).

[17] S. Calder *et al.*, Enhanced spin-phonon-electronic coupling in a 5*d* oxide, Nat. Commun. **6**, 8916 (2015).

[18] J. C. Slater, Magnetic effects and the hartree-fock equation, Phys. Rev. **82**, 538 (1951).

[19] H. Shinaoka, T. Miyake, and S. Ishibashi, Noncollinear Magnetism and Spin-Orbit Coupling in 5*d* pyrochlore oxide $Cd_2Os_2O_7$, Phys. Rev. Lett. **108**, 247204 (2012); Z. Hiroi, J. Yamaura, T. Hirose, I. Nagashima, and Y. Okamoto, Lifshitz Metal-insulator transition induced by the all-in/all-out magnetic order in the pyrochlore oxide $Cd_2Os_2O_7$, APL Mater. **3**, 041501 (2015).

[20] C. H. Sohn, H. Jeong, H. Jin, S. Kim, L. J. Sandilands, H. J. Park, K. W. Kim, S. J. Moon, D.-Y. Cho, J. Yamaura, Z. Hiroi, and T. W. Noh, Optical Spectroscopic Studies of the Metal-Insulator Transition Driven by All-InAll-Out Magnetic Ordering in 5*d* Pyrochlore $Cd_2Os_2O_7$, Phys. Rev. Lett. **115**, 266402 (2015).

[21] I. M. Lifshitz, Anomalies of electron characteristics of a metal in the high pressure region, Sov. Phys. JETP **11**, 1130 (1960).

[22] M. C. Jung, Y. J. Song, K. W. Lee, and W. E. Pickett, Structural and correlation effects in the itinerant insulating antiferromagnetic perovskite $NaOsO_3$, Phys. Rev. B **87**, 115119 (2013).

[23] S. Middey, S. Debnath, P. Mahadevan, and D. D. Sarma, $NaOsO_3$: A high Néel temperature 5*d* oxide, Phys. Rev. B **89**, 134416 (2014).

[24] Y. Du, X. Wan, L. Sheng, J. Dong, and S. Savrasov, Electronic structure and magnetic properties of $NaOsO_3$, Phys. Rev. B **85**, 174424 (2012).

[25] G. Kresse and J. Furthmüller, Efficient iterative schemes for *ab initio* total-energy calculations using a plane-wave basis set, Phys. Rev. B **54**, 11169 (1996).

[26] See Supplemental Material at http://link.aps.org/supplemental/10.1103/PhysRevB.94.241113 for additional computational details.

[27] M. K. Stewart, C. H. Yee, J. Liu, M. Kareev, R. K. Smith, B. C. Chapler, M. Varela, P. J. Ryan, K. Haule, J. Chakhalian, and D. N. Basov, Optical study of strained ultrathin films of strongly correlated $LaNiO_3$, Phys. Rev. B **83**, 075125 (2011).

[28] M. M. Qazilbash, J. J. Hamlin, R. E. Baumbach, L. Zhang, D. J. Singh, M. B. Maple, and D. N. Basov, Electronic correlations in the iron pnictides, Nat. Phys. **5**, 647 (2009).

[29] F. Aryasetiawan, M. Imada, A. Georges, G. Kotliar, S. Biermann and A. I. Lichtenstein, Frequency-dependent local interactions and low-energy effective models from electronic structure calculations, Phys. Rev. B **70**, 195104 (2004).

[30] A. J. Millis, A. Zimmers, R. P. S. M. Lobo, N. Bontemps, and C. C. Homes, Mott physics and the optical conductivity of electron-doped cuprates, Phys. Rev. B **72**, 224517 (2005).

[31] Q. Si, Iron pnictide superconductors: Electrons on the verge, Nat. Phys. **5**, 629 (2009).

[32] G. Giovannetti and M. Capone, Dual nature of the ferroelectric and metallic state in $LiOsO_3$, Phys. Rev. B **90**, 195113 (2014).

[33] J. M. Rondinelli, N. M. Caffrey, S. Sanvito, and N. A. Spaldin, Electronic properties of bulk and thin film $SrRuO_3$: Search for the metal-insulator transition, Phys. Rev. B **78**, 155107 (2008).

[34] P. Mohn, *Magnetism in the Solid State* (Springer, Berlin, 2006).

[35] L. Baldassarre, A. Perucchi, D. Nicoletti, A. Toschi, G. Sangiovanni, K. Held, M. Capone, M. Ortolani, L. Malavasi, M. Marsi, P. Metcalf, P. Postorino, and S. Lupi, Quasiparticle evolution and pseudogap formation in V_2O_3: An infrared spectroscopy study, Phys. Rev. B **77**, 113107 (2008).

[36] A. Damascelli, K. Schulte, D. van der Marel, M. Fäth, and A. A. Menovsky, Optical phonons in the reflectivity spectrum of FeSi, Physica B **230-232**, 787 (1997).

[37] S. Paschen, E. Felder, M. A. Chernikov, L. Degiorgi, H. Schwer, H. R. Ott, D. P. Young, J. L. Sarrao, and Z. Fisk, Low-temperature transport, thermodynamic, and optical properties of FeSi, Phys. Rev. B **56**, 12916 (1997).

[38] V. V. Mazurenko, A. O. Shorikov, A. V. Lukoyanov, K. Kharlov, E. Gorelov, A. I. Lichtenstein, and V. I. Anisimov, Metal-insulator transitions and magnetism in correlated band

insulators: FeSi and $Fe_{1-x}Co_xSi$, Phys. Rev. B **81**, 125131 (2010).

[39] T. Moriya, *Spin Fluctuations in Itinerant Electron Magnetism*, Springer Series in Solid-State Sciences (Springer, Berlin, 1985).

[40] J. Kübler, *Theory of Itinerant Electron Magnetism* (Oxford University Press, Oxford, UK, 2000).

[41] S. Khmelevskyi, First-principles modeling of longitudinal spin fluctuations in itinerant electron antiferromagnets: High Néel temperature in the V_3Al alloy, Phys. Rev. B **94**, 024420 (2016).

[42] S. K. Panda, I. Dasgupta, E. Şaşiğlu, S. Blügel, and D. D. Sarma, NiS—An unusual self-doped, nearly compensated antiferromagnetic metal, Sci. Rep. **3**, 2995 (2013).

[43] S. Gangopadhyay and W. E. Pickett, Interplay between spin-orbit coupling and strong correlation effects: Comparison of three osmate double perovskites Ba_2AOsO_6 (A = Na, Ca, Y), Phys. Rev. B **93**, 155126 (2016).

[44] M.-C. Jung and K.-W. Lee, Electronic structures, magnetism, and phonon spectra in the metallic cubic perovskite $BaOsO_3$, Phys. Rev. B **90**, 045120 (2014).